Supplement of Atmos. Chem. Phys., 15, 3629–3646, 2015
http://www.atmos-chem-phys.net/15/3629/2015/
doi:10.5194/acp-15-3629-2015-supplement

Atmospheric Chemistry and Physics Open Access

Supplement of

Chemical characterization of biogenic secondary organic aerosol generated from plant emissions under baseline and stressed conditions: inter- and intra-species variability for six coniferous species

C. L. Faiola et al.

Correspondence to: T. M. VanReken (vanreken@wsu.edu)

AMS Data Analysis

The m/z values used in UMR analysis were 12, 13, 15, 17, 18, 25, 26, 27, 29, 30, 31, 37, 38, 41, 42, 43, 44, 45, 50, 51, 52, 53, 54, 55, 56, 57, 58, 59, 62, 63, 64, 65, 66, 67, 68, 69, 70, 71, 72, 73, 74, 77, 78, 79, 80, 81, 82, 83, 84, 85, 89, 91, 92, 93, 94, 95, 96, 97, 98, 99, 100, 101, 103, 105, 106, 107, 108, 109, 110, 111, 113, 114, 115, 117, 119, 120, 121, 123, 125, 127, 129, 131, 134, 135, 137, 152, 155, 157, 202.

To perform HR-AMS data analysis, it is necessary to carefully correct the particle signals that have significant air interferences. To account for some of these interferences, HEPA particle filters were placed in the sampling line at the beginning and end of each experiment for a minimum of ten runs. Using these filter runs, adjustments were made to the UMR fragmentation table for m/z 15, 16, 29, and 44 and to the high resolution (HR) fragmentation table for ions $^{15}N^+$, O^+, and CO_2^+. When performing elemental analysis, extra care is required to identify and remove additional interferences for a few HR ions (Aiken et al., 2008). For example, the HR ions at O^+, HO^+, and H_2O^+ are produced from organic material in particles, but also have significant interferences with particulate water. Particulate water was reduced by placing a gas sample dryer (Perma Pure, model MD-110) along the inlet, but it is very difficult to eliminate all particulate water. Consequently, the organic particle contribution to these signals was constrained using the organic particle CO_2^+ signal as suggested by Aiken et al. (2008).

Another important ion, the CO^+ ion (exact mass 27.9949), is often overwhelmed by the very large neighboring N_2^+ ion (exact mass 28.0061). The N_2^+ air ion is still very large even though the vacuum in the HR-AMS dilutes gas phase molecules by a factor of 10^7 relative to aerosol species (Allan et al., 2004). Evaluations of the organic particle contribution to CO^+ have generally found that the ratio of organic particulate CO^+ to organic particulate CO_2^+ is approximately one (Aiken et al., 2008). We investigated this interference using p-ToF data to separate the CO^+ ion from the air N_2^+ signal at m/z 28; fourteen of the thirty-four total experiments had high quality p-ToF signal that allowed us to directly calculate the organic CO^+/ CO_2^+ ratio. The tail of the air N_2^+ peak was subtracted from the CO^+ signal before integrating the peaks and calculating the ratio. The organic CO^+/ CO_2^+ ratio ranged from 0.79-3.04 with an average value of 1.6 +/- 0.6%. The pre-treatment and negative control experiments (N=8) had ratios close to the literature value of ~1, with an average of 1.1 +/- 0.3 (mean +/- one standard deviation). The stress experiments (N=6) had a higher ratio, with an average of 2.2 +/- 0.6. Sample p-ToF spectra for both pre-treatment and post-treatment conditions are shown in Supplementary Figure S-1. These results were used to inform corrections for experiments that did not have useful p-ToF data. For pre-treatment and negative control experiments where the ratio could not be directly calculated (N=14), a default value of 1 was used. For stress experiments where the ratio could not be directly calculated (N=6), elemental analysis was performed twice, once using the average

measured stress value of 2.2 and once using the default literature value of 1. This was done to ensure the data treatment did not skew overall conclusions. Final results are shown using a ratio of 2.2.

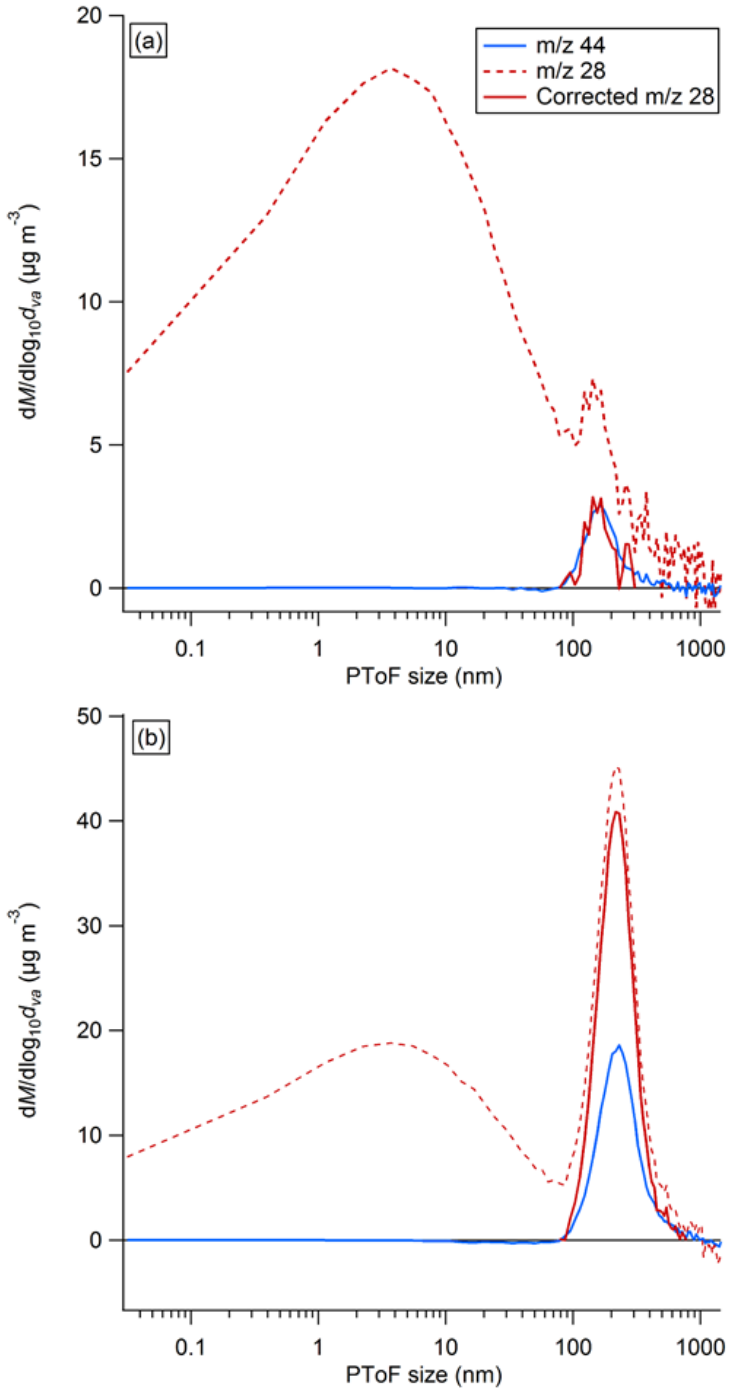

Figure S-1: Sample p-ToF data for m/z 28 and 44 for two experiments. (a) baseline experiment using *Picea pungens* (blue spruce) emissions, (b) stress experiment using both *Pseudotsuga menziesii* and *Abies grandis* emissions (fir mix). The ratio of m/z 28 to m/z 44 was significantly different between baseline and stress experiments. This difference persists for all experiments where p-ToF data was available.

Additional UMR Comparisons

SOA spectra generated the same year were more similar to one another than SOA generated in different years. We hypothesize that some of difference between years could be attributed to differences in tree types and tree maturity from 2012 to 2013. In the 2012 experiments, only *Pinus ponderosa* and *Pinus aristata* were used and they were 2-3 years of age at the time of the experiments. In contrast, in 2013 all tree types except for *Pinus ponderosa* were used and most of the experiments were performed with trees that were 1 year of age. Furthermore, two of the 2012 PreT/PostT experiments were performed in October after the plants had already entered their winter dormancy period. As a result, there could have been confounding stress effects impacting SOA composition in four of the six total 2012 biogenic SOA spectra. However, we are unable to state with certainty why there were differences in SOA spectra between different years.

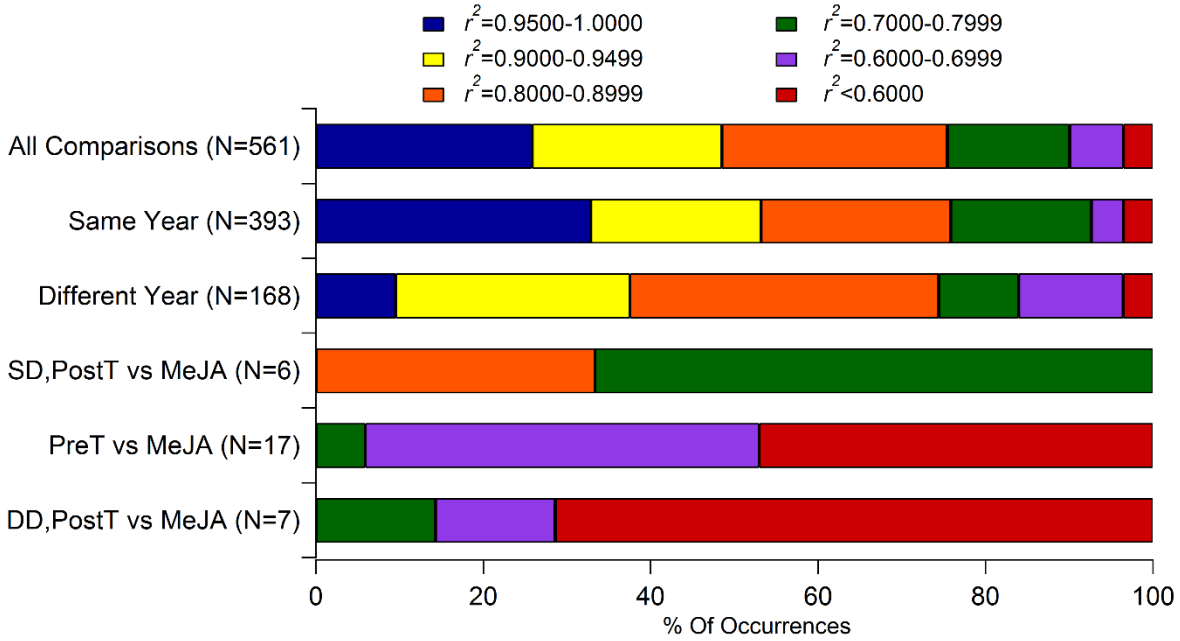

Figure S-2: Distribution of correlations classified by type of comparison. X-axis is the % of total occurrences within a given correlation range for each experiment classification. Each horizontal bar denotes the type of comparison where the N value in parentheses refers to the total number of comparisons within that classification. SD,PostT=Post-Treatment where treatment and SOA growth experiment occurred on the same day; DD,PostT=Post-treatment spectra where treatment and SOA growth experiment occurred on subsequent days; MeJA=comparisons with SOA spectra of aerosol formed from the oxidation of a methyl jasmonate standard. The bottom three horizontal bars comparing the standard MeJA SOA spectra to different types of biogenic SOA are discussed in Section 3.4 in the main text.

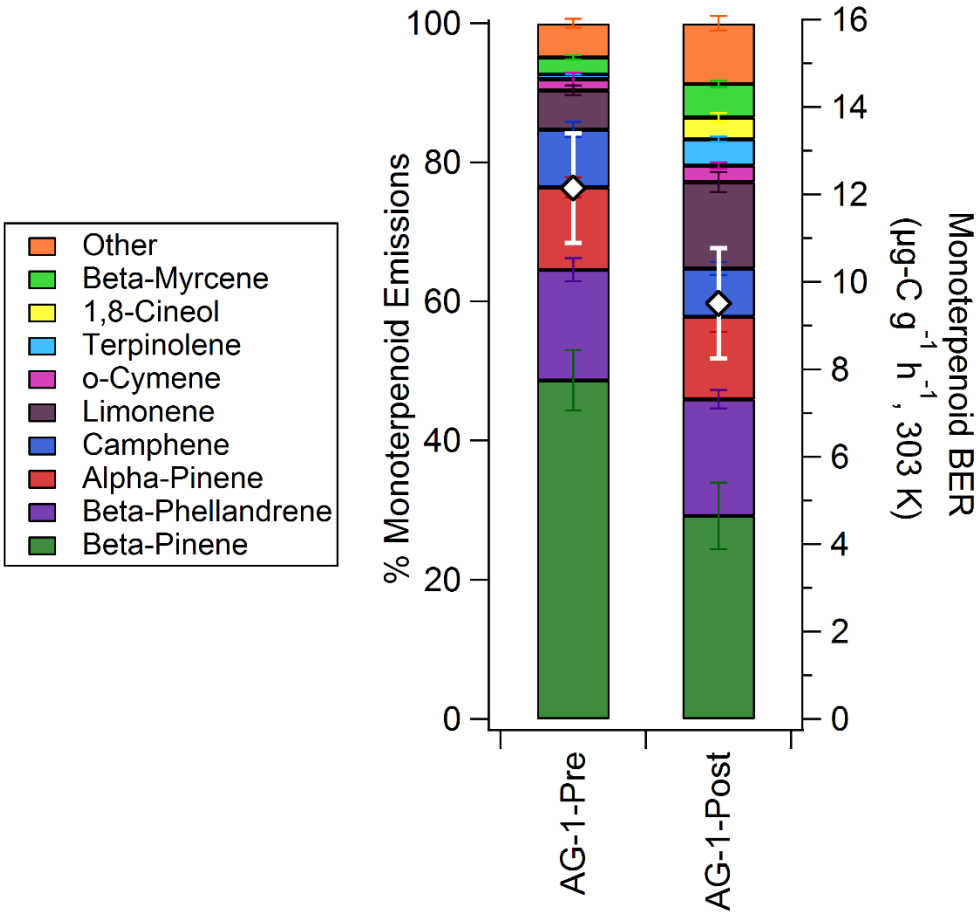

Figure S-3: BVOC profile while loading aerosol growth chamber for experiments with *Abies grandis* (AG) emissions from experiment AG-1. Left axis is the percent of total monoterpenoid compound emissions. The diamonds correspond to the right axis, which shows the average basal emission rate (BER, 303 K) during the aerosol chamber loading period. The error bars represent the standard deviation.

Comparison of Biogenic SOA

Figure S-4 shows the normalized AMS spectrum of SOA generated from the dark ozonolysis of alpha-pinene. Alpha-pinene has been used as a model compound for investigations of biogenic SOA by the aerosol community. It is provided here for comparison with a pre-treatment SOA spectrum generated from the oxidation of real plant emissions (Figure 7, main text). The dominant peaks in the two spectra are similar, with *m/z* 43 contributing the greatest organic signal. This is true for most SOA generated from monoterpene precursors in laboratory chambers (Chhabra et al., 2010, 2011). Other dominant peaks in both spectra are m/z 29, 44, 27, 41, 55, 42, 26, and 53. The relative contribution of these peaks between the spectra does vary slightly and there are some major peaks in the alpha-pinene SOA that are not as prominent in the AG-2-Pre spectrum. Some of this variation could be due to differences in fragmentation between AMS instruments, and/or differences in chemistry between chambers. For example, one difference between the two studies is that OH scavengers were used in the Bahreini et al. (2005). This limits our ability to perform a quantitative comparison between alpha-pinene SOA spectra and the biogenic SOA spectra presented in this paper.

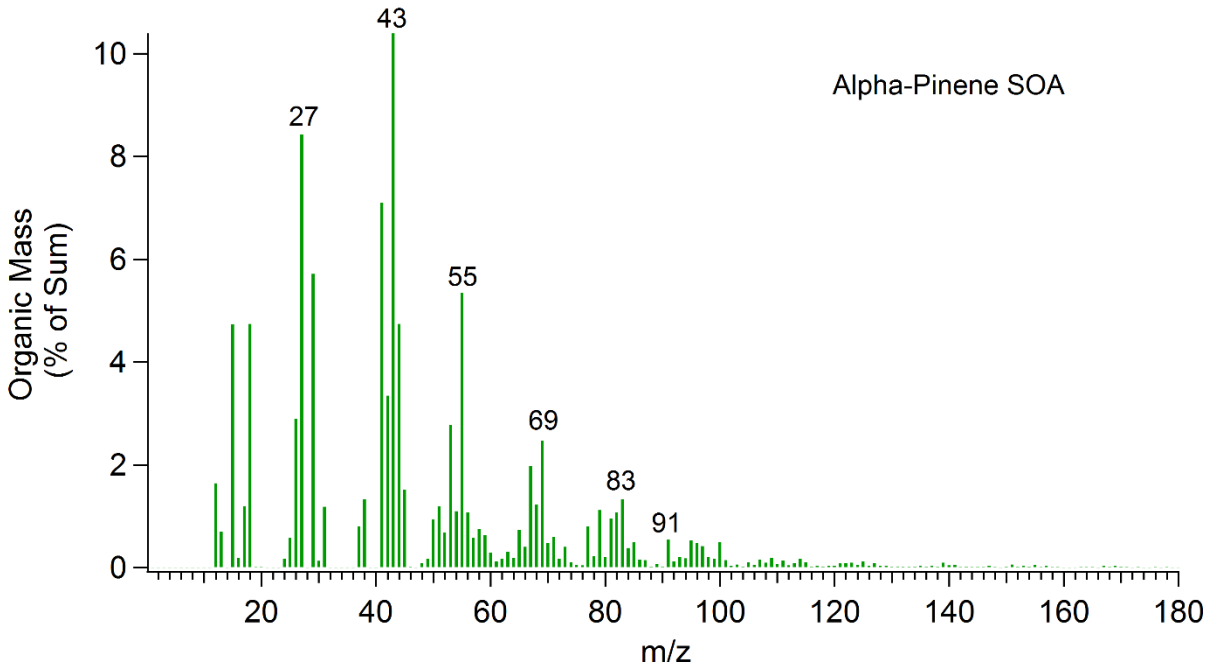

Figure S-4: AMS spectrum of alpha-pinene SOA generated from dark ozonolysis reactions (Bahreini et al., 2005).

References

Aiken, A. C., DeCarlo, P. F., Kroll, J. H., Worsnop, D. R., Huffman, J. A., Docherty, K. S., Ulbrich, I. M., Mohr, C., Kimmel, J. R., Sueper, D., Sun, Y., Zhang, Q., Trimborn, A., Northway, M., Ziemann, P. J., Canagaratna, M. R., Onasch, T. B., Alfarra, M. R., Prevot, A. S. H., Dommen, J., Duplissy, J., Metzger, A., Baltensperger, U., and Jimenez, J. L.: O / C and OM / OC Ratios of Primary, Secondary, and Ambient Organic Aerosols with HighResolution Time-of-Flight Aerosol Mass Spectrometry, Environ. Sci. Technol., 42, 4478–4485, doi:10.1021/es703009q, 2008

Allan, J. D., Delia, A. E., Coe, H., Bower, K. N., Alfarra, M. R., Jimenez, J. L., Middlebrook, A. M., Drewnick, F., Onasch, T. B., and Canagaratna, M. R.: A generalised method for the extraction of chemically resolved mass spectra from Aerodyne aerosol mass spectrometer data, J. Aerosol Sci., 35, 909–922, 2004.

Bahreini R., Keywood, M. D., Ng, N. L., Varutbangkul, V., Gao, S., Flagan, R. C., Seinfeld, J. H., Worsnop, D. R., and Jimenez, J. L.: Measurements of secondary organic aerosol from oxidation of cycloalkenes, terpenes, and m-xylene using an Aerodyne aerosol mass spectrometer, Environ. Sci. Technol., 39, 5674–5688, 2005.

Chhabra, P. S., Flagan, R. C., and Seinfeld, J. H.: Elemental analysis of chamber organic aerosol using an aerodyne high-resolution aerosol mass spectrometer, Atmos. Chem. Phys., 10, 4111–4131, doi:10.5194/acp-10-4111-2010, 2010.

Chhabra, P. S., Ng, N. L., Canagaratna, M. R., Corrigan, A. L., Russell, L. M., Worsnop, D. R., Flagan, R. C., and Seinfeld, J. H.: Elemental composition and oxidation of chamber organic aerosol, Atmos. Chem. Phys., 11, 8827–8845, doi:10.5194/acp-11-8827- 2011, 2011.